Proceedings of the Tenth Pacific Conference on Earthquake Engineering
Building an Earthquake-Resilient Pacific
6-8 November 2015, Sydney, Australia

Estimating the accuracy of single-mode pushover analysis for unreinforced masonry buildings with flexible diaphragms

Y. Nakamura, H. Derakhshan & M.C. Griffith

University of Adelaide, Adelaide, Australia.

G. Magenes

University of Pavia and EUCENTRE, Pavia, Italy.

ABSTRACT: Nonlinear static analyses of unreinforced masonry buildings are typically carried out assuming a single-mode response of the structure. While this assumption is appropriate when the floor and the roof diaphragms are rigid in their own planes, many existing unreinforced masonry buildings have flexible timber diaphragms, for which the applicability of a single-mode pushover analysis becomes questionable.

This paper explores whether the accuracy of a single-mode pushover analysis can be estimated from the results of the pushover analysis itself. From the theoretical consideration, a key parameter that reflects the validity of the single-mode pushover analysis is shown to be the sensitivity of the analysis to the control node location, and a measure of the control node sensitivity is proposed. Preliminary parametric studies conducted on idealised single-storey systems and a two-storey building show that the proposed measure can provide an indicative error of the single-mode pushover analysis.

1 INTRODUCTION

Nonlinear static (pushover) methods have become widely used for the seismic demand estimation of buildings, with various forms of the method specified in Eurocode 8 (CEN 2004), ATC-40 (ATC 1996) and ASCE 41-13 (ASCE 2014). In association with the advances in the development of efficient numerical tools, the use of pushover analysis has also become common for the evaluation of unreinforced masonry (URM) buildings (Magenes and Penna 2009).

The pushover methods currently used for masonry buildings almost exclusively correspond to the single-degree-of-freedom (SDOF) representation of the structure, in which the pushover analysis is carried out using invariant lateral forces. Typically, the lateral forces are assumed to be proportional to mass (uniform displacement shape) or to mass multiplied by a linear (inverted triangular) shape along the height of the building. The former approximates the soft-storey behaviour, while the latter is more appropriate when the inelastic deformations are distributed throughout the building or when the walls behave as weakly coupled cantilevers. Such single-mode pushover (SPO) analysis is known to be an acceptable approximation for low-rise regular buildings with rigid diaphragms. However, existing URM buildings often have flexible timber floor and roof diaphragms, and several studies have questioned the indiscriminate use of the SPO analysis when the diaphragms are flexible (Costley and Abrams 1995; Mendes and Lourenço 2009). Although refined pushover methods, for example a multi-mode procedure (Chopra and Goel 2002), can be extended to buildings with flexible diaphragms, it is important to be able to estimate when a SPO analysis can be applied with sufficiently accurate results. This is particularly so for URM buildings, of which the majority may be considered to be simple structures, for which correspondingly simple analysis procedures are preferred in practice.

In this paper, the theoretical background of the SPO analysis is firstly summarised, showing that a reliable SPO analysis should be independent of the control node location. The differences in the predicted responses obtained using different control nodes are considered to reflect the inaccuracy of the SPO analysis, and a measure of the control node sensitivity is proposed. Parametric analyses on idealised single-storey systems and a two-storey building suggest that the proposed measure can provide an indicative error of the SPO analysis.

2 THEORETICAL BACKGROUND

The theoretical basis of the SPO analysis relies on the assumption of an invariant deflected shape $\boldsymbol{\phi}$ of the structure throughout the excitation (Fajfar and Gašperšič 1996; Krawinkler and Seneviratna 1997), which is used to reduce the multi degree of freedom (MDOF) structure to an equivalent SDOF system.

Consider the nonlinear MDOF equation of motion,

$$\boldsymbol{m}\ddot{\boldsymbol{u}} + \boldsymbol{c}\dot{\boldsymbol{u}} + \boldsymbol{f_s}(\boldsymbol{u}, \dot{\boldsymbol{u}}) = -\boldsymbol{m\iota}\ddot{u}_g(t) \tag{1}$$

where $\boldsymbol{m}$ and $\boldsymbol{c}$ are the mass and the damping matrices respectively, $\boldsymbol{u}$ is the relative displacement vector, $\boldsymbol{f_s}$ is the vector of nonlinear resisting forces, $\boldsymbol{\iota}$ is the influence vector of the ground motion and $\ddot{u}_g$ is the ground acceleration. Introducing the assumption of the invariant displacement profile,

$$\boldsymbol{u} = \boldsymbol{\phi} q(t) \tag{2}$$

Substituting Eq. 2 into Eq. 1, pre-multiplying by $\boldsymbol{\phi}^{\mathrm{T}}$ and simplifying the equation in a manner analogous to the standard modal decomposition (Chopra 2007) gives the equation of motion of the equivalent SDOF system,

$$\ddot{D} + 2\xi\omega\dot{D} + \frac{F_s(D,\dot{D})}{L} = -\ddot{u}_g(t) \tag{3}$$

where $F_s = \boldsymbol{\phi}^{\mathrm{T}}\boldsymbol{f_s}$, $L = \boldsymbol{\phi}^{\mathrm{T}}\boldsymbol{m\iota}$, $D = \frac{q}{\Gamma}$, and $\Gamma = \frac{\boldsymbol{\phi}^{\mathrm{T}}\boldsymbol{m\iota}}{\boldsymbol{\phi}^{\mathrm{T}}\boldsymbol{m\phi}}$. The damping term is expressed by the initial frequency ω and the damping ratio ξ corresponding to the assumed displacement shape, defined so that $\frac{\boldsymbol{\phi}^{\mathrm{T}}\boldsymbol{c\phi}}{\boldsymbol{\phi}^{\mathrm{T}}\boldsymbol{m\phi}} = 2\xi\omega$.

The SPO analysis approximates the force-displacement relationship of the equivalent SDOF system (F_s/L-D) by the base shear – control node displacement (V_b-u_k) relationship (pushover curve) of a static pushover analysis of the structure subjected to incremental lateral forces proportional to $\boldsymbol{m\phi}$ (Fajfar and Gašperšič 1996). It should be noted that the pushover curve is not a unique property of the structure as it depends on the choice of $\boldsymbol{\phi}$ and the location of the control node. The conversion between the pushover curve and F_s/L-D (capacity curve) of the equivalent SDOF system is given by

$$D = \frac{u_k}{\Gamma\phi_k} \tag{4}$$

$$\frac{F_s}{L} = \frac{V_b}{\Gamma L} \tag{5}$$

In the N2 method, the displacement profile is normalised to the control node location, i.e. ϕ_k=1.

The capacity curve is typically simplified by a bilinear idealisation to enable the solution of Eq. 3. Eq. 3 can be solved rigorously by the nonlinear time history analysis (NTHA) of the equivalent SDOF system. Alternatively, the peak value of D may be obtained using approximate techniques such as the equivalent linearisation (Capacity Spectrum Method), the use of the modification factors on the elastic displacement (Displacement Coefficient Method) or the use of the inelastic spectrum (N2 method). Once the peak value of D is obtained, Eq. 4 can be inverted to obtain the peak displacement estimate of the control node. The results of the pushover analysis at the peak control node displacement gives the approximate peak seismic demands (e.g. displacements, inter-storey drifts, member chord rotations) of the structure.

3 MEASURE OF CONTROL NODE SENSITIVITY

A pushover analysis satisfying Eq. 2 is independent of the control node location. This can be seen by considering analyses with the same assumed displacement shape, but using two different control nodes j and k. The only difference between the two analyses is the displacement definition of the equivalent SDOF systems, D_j and D_k, as given by Eq. 4. If Eq. 2 is re-written as

$$\frac{u_j}{u_k} = \frac{\phi_j}{\phi_k} \tag{6}$$

and substituted into D_j,

$$D_j = \frac{u_j}{\Gamma\phi_j} = \frac{u_k}{\Gamma\phi_j}\frac{\phi_j}{\phi_k} = D_k = D \quad (7)$$

The two equivalent SDOF systems are hence identical to each other, and the same peak displacement will be obtained when Eq. 3 is solved. Similar consideration shows that the structural responses (e.g. displacement, inter-storey drifts) are also identical when $\boldsymbol{\phi}$ reflects the exact displacement shape.

However, the SPO analysis is generally *not* independent of the control node because (1) a building entering in the nonlinear response regime continuously changes its displacement shape, and (2) the multi-mode behaviour becomes prominent as the diaphragm flexibility increases, neither of which can be captured by a single invariant displaced shape. If a control node k is used in the SPO analysis, the degree to which the predicted responses depend on the choice of the control node may be expressed in the form of error as (referred to as control node sensitivity, CS)

$$CS = \left|\frac{r_k}{r_j} - 1\right|, \; j \neq k \quad (8)$$

where r_k is a response of interest from the pushover analysis using the reference control node k, and r_j is the corresponding result using some other control node $j \neq k$. The value of CS varies depending on the response parameter used (e.g. displacements, inter-storey drifts, chord rotations), the selected control node locations, and for the different locations/members of the structure. If several control nodes are used for the additional analyses (i.e. for node j in Eq. 8), the maximum value of CS can be used as the control node sensitivity.

An invariant displacement shape could approximate the nonlinear displacements if the structure is appropriately designed, for instance by distributing the seismic demand uniformly throughout the structure, so that the likely displacement shape of the structure is known. However, in most cases of existing structures, the distribution of the nonlinear deformation demand cannot be identified a priori, and the assumption of a fixed displacement shape is generally incorrect. This problem has led in the past to the proposal of adaptive pushover methods (Galasco et al. 2006) where the evolving nature of the displacement shape is accounted for in the pushover procedure. Nevertheless, for a SPO analysis to give correct results, Eq. 2 must be valid, so that the pushover analysis will give consistent results irrespective of the choice of the control node. Hence it may be supposed that a correlation exists between the control node sensitivity and the accuracy of the SPO analysis and Eq. 8 to provide an indicative measure of the accuracy of the non-adaptive, fixed shape SPO analysis. This premise is investigated in the following section.

4 NUMERICAL ANALYSIS

4.1 *Idealised single-storey system*

A parametric analysis was conducted using idealised single-bay single-storey systems with one-way stiffness and strength eccentricities (Fig. 1(a), 1(b)). Simple single-storey systems representing the most basic response characteristics of buildings with flexible diaphragms were used in order to eliminate the uncertainties associated with the height-wise distribution of the pushover forces and to enable the rigorous solution of the equation of motion of the equivalent SDOF system. Therefore the inaccuracy of the SPO analysis resulting from the diaphragm flexibility can be isolated. The parameters of the model are defined by (1) plan dimensions L_x and L_y, (2) total mass, (3) period of the rigid diaphragm system T_y, (4) ratio of the uncoupled torsional to translational frequencies of the rigid diaphragm condition Ω_θ, (5) stiffness eccentricity ε_{sx}, (6) strength eccentricity ε_{px}, (7) force reduction factor under the rigid diaphragm condition in the direction of excitation R_y, (8) ratio of strengths in the orthogonal direction to the direction of excitation R_F, (9) fraction of masses attributed to the walls (ρ_{w1}, ρ_{w2} etc.) and the diaphragm ρ_d, and (10) fundamental period of the diaphragm as a shear beam T_d. The systems used in this study had the following constant properties; L_x=12 m, L_y=18 m, total mass of 25 tons, T_y = 0.35 s, Ω_θ = 1, R_F = 1, ρ_{w1}=ρ_{w2}=ρ_{w3}=ρ_{w4} = 0.225, ρ_d=0.1 and the constant modal damping ratio of 5%. The inelastic behaviour of the spring was represented by a Takeda model. The wall masses were lumped at the locations of wall springs, while the diaphragm mass was

distributed across the diaphragm elements. The diaphragms were modelled by elastic membrane elements, with each line of nodes constrained to move together in each orthogonal direction, so that the diaphragm deformation was governed by its shear modulus calculated from T_d. The stiffness eccentricity ε_{sx} amounted to $0.3L_x$. The strength parameters were varied as shown in Table 1 to create systems with two levels of yielding (R_y=2.5 or 4), that had either a symmetric distribution of wall strength (ε_{px}=0), or the strength eccentricity equal to the stiffness eccentricity ($\varepsilon_{px} = \varepsilon_{sx}$). The diaphragm period was varied between 0.01 s and 2 s.

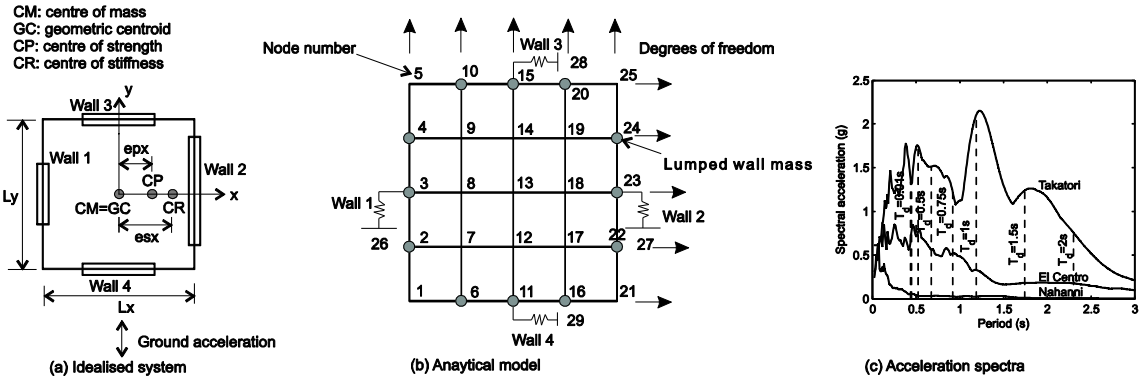

Figure 1. Idealised model and ground motions used in the analysis.

Table 1. Models used in the analysis

Model	R_y	ε_{px}
M1	2.5	0.0
M2	2.5	0.3
M3	4	0.0
M4	4	0.3

Three unscaled ground motions of different frequency content and intensities were used in the analysis. The ground motions were (1) El Centro earthquake recorded on 19th May 1940, (2) Nahanni earthquake recorded on 23th of December 1985, and (3) Kobe earthquake recorded at Takatori station on 16th January 1995. Figure 1(c) shows the 5% damped elastic spectra of the records together with the fundamental periods of the considered systems.

The NTHA of the system was considered to provide the "exact" peak displacements, $\boldsymbol{u}_{THA}$. As the variation of pushover forces along the height of the building was irrelevant for the single-storey model, the SPO analysis was conducted using pushover forces proportional to the distribution of mass in the direction of loading. The response of the equivalent SDOF system was calculated rigorously by solving the nonlinear equation of motion (Eq. 3) using the bilinearised F_s/L-D relationship, and the peak displacement of the equivalent SDOF system was converted back to the control node displacement by inverting Eq. 4. The pushover analysis at that control node displacement gave the estimated peak displacements, $\boldsymbol{u}_{SPO}$.

The accuracy of the SPO analysis was measured by the peak displacement error (PDE)

$$PDE = \frac{u_{SPO}}{u_{THA}} - 1 \tag{9}$$

which were evaluated for the displacements at wall 1, wall 2 and the diaphragm mid-span.

The control node sensitivity (CS) defined in Eq. 8 were calculated from the displacements obtained by the SPO analysis with the reference control node at the diaphragm mid-span, and the additional analyses using control nodes on wall 1 and wall 2. The maximum values of CS were then recorded for wall 1, wall 2 and the diaphragm mid-span. Note that the CS values are calculated solely from pushover analysis, while the PDE expresses the accuracy of SPO with respect to NTHA.

Figure 2 shows the typical displacement predictions of SPO analysis when the control node is varied between wall 1, wall 2 and the diaphragm mid-span (shown for model M3 subjected to the El Centro record). The predictions clearly show the increased sensitivity to the control node location as the diaphragm flexibility increases.

Figure 3 shows the values of CS and the corresponding PDE. Also indicated on the plots are the equality relationship between the absolute value of the PDE and the CS. A good correlation between the PDE and the CS can be observed for the El Centro record, with the CS providing an indicative upper-bound error of the SPO analysis. This indicates that the exact responses tend to lie within the range of responses predicted by the SPO analyses using different control nodes, as confirmed in Figure 2. For the Nahanni and the Takatori records, the correlation is not as clear as for the El Centro record. Large overestimations can be observed for both records when CS is in the range of 0.3 to 0.6, which imply that the SPO analysis tends to be conservative, regardless of the location of the control node. In fact, a SPO analysis is likely to overestimate the actual responses when the diaphragm becomes flexible because the analysis assumes the majority of the seismic mass (the value depends on the assumed displacement shape) to participate in a single mode, while the actual response is governed by a multi-mode behaviour in which some out-of-phase cancelling of responses would occur. The underestimation errors of the SPO analysis, however, are consistently bound by the CS for all records.

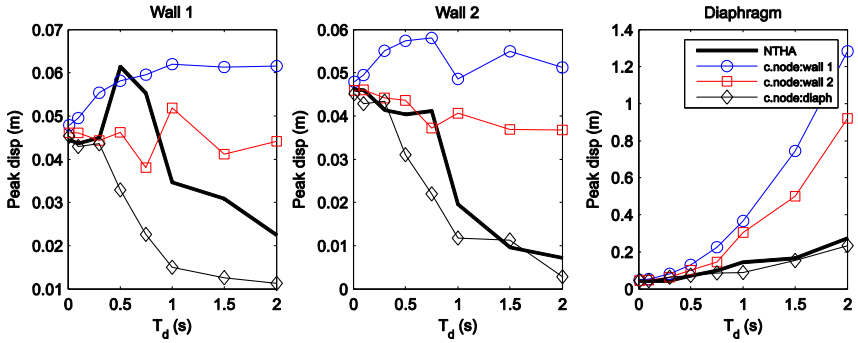

Figure 2. Peak displacement predictions by SPO analysis using different control nodes for M3 subjected to El Centro accelerogram.

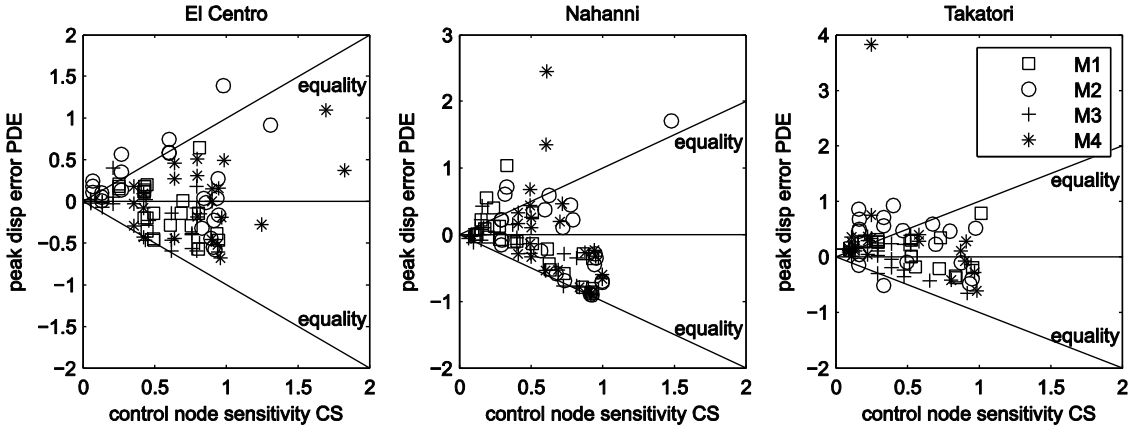

Figure 3. Correlation between peak displacement error and the control node sensitivity.

4.2 *Two-storey stone masonry building*

The use of the control node sensitivity in gauging the accuracy of the SPO analysis is further investigated using a full-scale stone masonry building with strengthened timber floor and roof, which was tested under shake-table excitations at EUCENTRE (Magenes et al. 2014). The building was subjected to the 1979 Montenegro earthquake measured at the Ulcinj-Hotel Albatros station, scaling the peak acceleration from 0.06 g to 1.16 g. The building was modelled using TREMURI (Lagomarsino et al. 2013) with each wall represented by the equivalent frame idealisation of their in-plane behaviour. The out-of-plane wall behaviour was not explicitly modelled. The deformable lengths of the equivalent frames (i.e. piers and spandrels) were modelled using the macroelement formulation

(Penna et al. 2014), which accounts for the axial-rocking interaction and shear-softening behaviours of URM. Each diaphragm was approximately represented by four elastic membrane finite elements to capture its vibrational behaviour (Figure 4), with the floor mass distributed to the perimeter walls and the diaphragm centre nodes based on simple tributary area consideration under lateral (inertial) loading. Additional static forces were applied on the walls to ensure the correct gravity stresses. This modelling approach was validated against the test data, with an acceptable accuracy (Fig. 5).

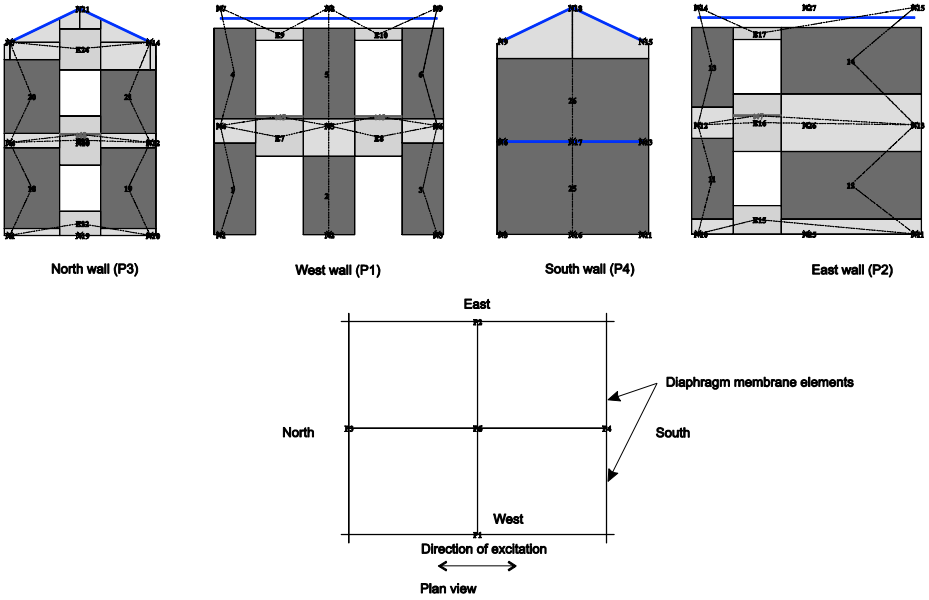

Figure 4. TREMURI model of tested building.

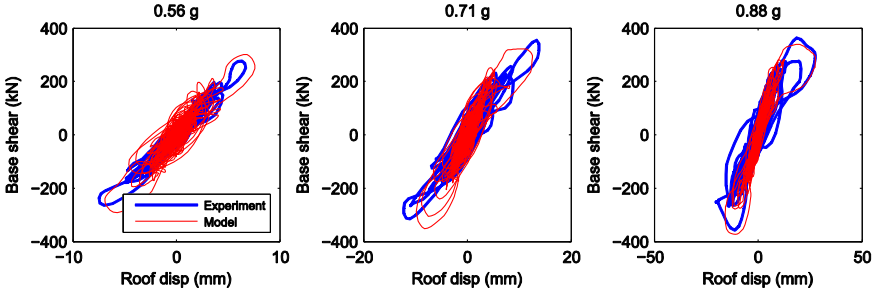

Figure 5. Comparison of numerical model against test data for 0.56 g to 0.88 g (penultimate) excitation levels.

Using the validated model, the diaphragm stiffness was reduced to 1.0, 0.75, 0.5 and 0.25 times the as-built configuration in order to simulate diaphragms of increasingly flexible constructions. The NTHA was conducted for each diaphragm configuration subjected to the 0.71 g and 0.88 g excitations. These analyses were considered to give the "exact" responses of the buildings for the purpose of assessing errors in the SPO analysis.

The SPO analyses were conducted using pushover forces proportional to mass and mass multiplied by a linear profile along the height of the structure. These two profiles are often considered to envelope the actual inelastic response (Galasco et al. 2006). Instead of rigorously solving the equation of motion of the equivalent SDOF system, the target displacement was estimated by the formulation of the N2 method (Vidic et al. 1994; Fajfar 1999). The CS for the displacements and the inter-storey drifts at each level of the west wall, east wall, and the diaphragm mid-spans were calculated using the roof mid-span as the reference control node, with the additional analyses conducted using the control nodes at the roof levels of the two longitudinal walls.

Figure 6 shows the PDE and the peak inter-storey drift errors (IDE), which is defined analogously to Eq. 9 using inter-storey drifts, against the corresponding CS for the uniform and the linear displacement profiles. For the uniform displacement shape, the CS correlates well with both the PDE and the IDE. As observed for the idealised single-storey system, the CS can be seen to approximate the indicative upper-bound error of the analysis. For the linear displacement shape, the poor

correlation is attributed to the actual response of the upper-storey west wall and the diaphragm not being bound by the SPO analyses with different control nodes (Fig. 7). However, for both assumed displacement shapes, the underestimation is again well bound by the CS and the SPO analysis generally tends to overestimate the "exact" NTHA responses.

An interest observation can be made regarding Figure 7, by noting that the three different predictions correspond to the same pushover analysis. The differences between them arise from the different levels of inelastic deformation depending on the control node location. Hence they indicate the progression of the nonlinear displacement under the pushover analysis conducted assuming a linear displacement shape. It can be seen that the analysis initially indicate larger upper storey deformation (for control node on east wall), but with an increased loading, the damage becomes concentrated at the ground storey (slight unloading takes place for the west wall). Hence even when the linear displacement is assumed, the pushover analysis ultimately indicates the concentration of inelastic damage at the ground storey, which is more consistent with the NTHA results, for which a uniform displacement shape may be considered more appropriate.

It may be noted that the SPO analysis does not converge to the exact response as the CS becomes small. Even for the uniform displacement shape, the PDE and the IDE of approximately 20% to 50% can be observed when the CS becomes negligible. This error is attributed to the inaccuracies inherent in the bilinear idealisation of the pushover curve and the empirical formulation used to estimate the peak displacement.

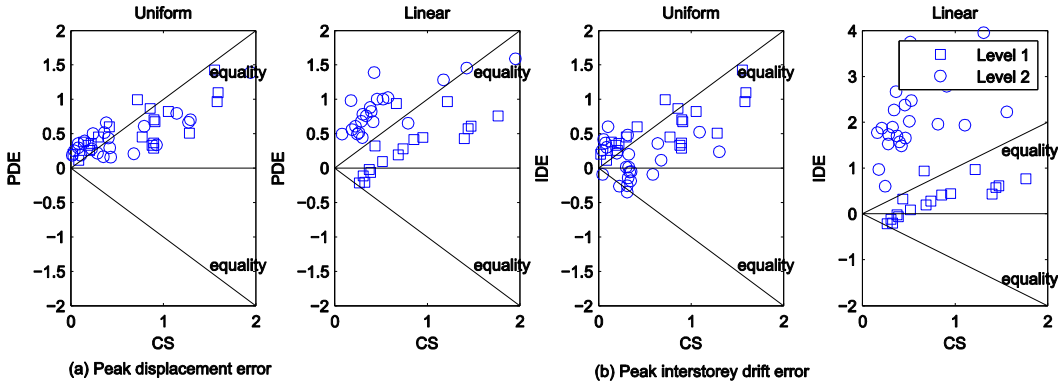

Figure 6. Correlation between control node sensitivity and peak displacement and interstorey drift errors.

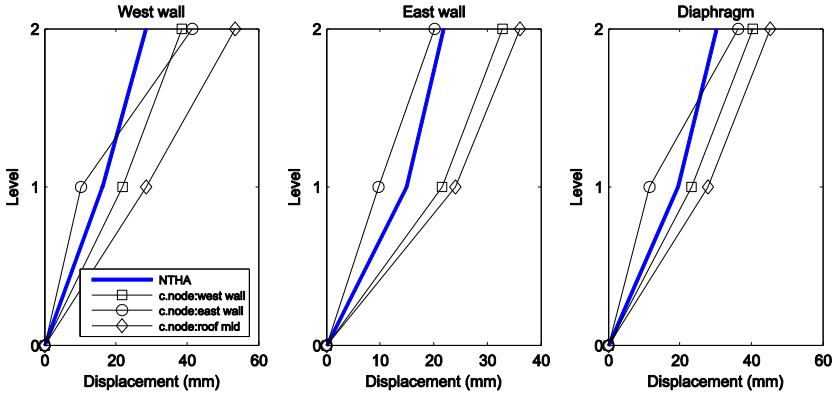

Figure 7. Comparison of NTHA of building model with diaphragm stiffness 0.5 times the as-built condition subjected to the 0.85 g excitation, with pushover analyses using linear displacement shape. The upper-storey displacements of the NTHA fall outside the predictions of the SPO analyses using different control nodes.

5 CONCLUSIONS

In this paper, a measure for estimating the accuracy of a single-mode pushover analysis was investigated based on the sensitivity of the pushover analysis predictions to the variations in the control node location. From the limited number of analyses carried out, the proposed measure of the control node sensitivity was generally found to correlate with the accuracy of the SPO analysis.

Provided that the displacement shape assumed in the pushover analysis was appropriate (i.e. consistent with the dominating failure mechanism) and several different control nodes are used, for example at the flexible and stiff walls and the roof mid-span, the SPO analysis tended to envelope the exact responses. In such cases, the proposed measure provided the upper-bound errors of the SPO analysis. Even when the SPO analyses did not envelope the exact response, they generally provided conservative estimates of the responses. Notably, the underestimation error was consistently bound by the proposed measure. Therefore, limiting the control node sensitivity to an acceptable value could be one of the requirements needed to avoid unsafe use of the SPO analysis for URM buildings with flexible diaphragms.

ACKNOWLEDGEMENTS

This work was supported by the Australian Research Council, through the grant DP120100848. The first author received financial support through the Australian Postgraduate Award. The authors would like to thank Dr. Senaldi from EUCENTRE for her suggestions on the numerical modelling of the experimentally tested building.

REFERENCES:

ASCE. 2014. Seismic evaluation and retrofit of existing buildings ASCE/SEI 41-13. *American Society of Civil Engineers*, Reston, Virginia.

ATC. 1996. ATC-40: Seismic evaluation and retrofit of concrete buildings, volume 1. *Applied Technology Council*, Redwood City, California.

CEN. 2004. EC8-1 – Eurocode 8: design of structures for earthquake resistance – part 1: general rules, seismic actions and rules for buildings. EN1998-1:2004. *CEN*. Brussels.

Chopra AK., Goel RK. 2002. A modal pushover analysis procedure for estimating seismic demands for buildings. *Earthquake Engineering and Structural Dynamics*. 31, 561 – 582.

Chopra AK. 2007. Dynamics of structures - theory and applications to earthquake engineering, third edition. *Pearson Prentice Hall*. Upper Saddle River, New Jersey.

Costley AC., Abrams DP. 1995. Dynamic response of unreinforced masonry buildings with flexible diaphragms, SRS No. 695. *University of Illinois at Urbana-Champaign*, Illinois.

Fajfar P., Gaspersic, P. 1996. The N2 method for the seismic damage analysis of RC buildings. *Earthquake Engineering and Structural Dynamics*. 24. 31 – 46.

Fajfar P. 1999. Capacity spectrum method based on inelastic demand spectra. *Earthquake Engineering and Structural Dynamics*. 28. 979 – 993.

Galasco A., Lagomarsino S., Penna A. 2006. On the use of pushover analysis for existing masonry buildings. *Proc. of 1st European Conference on Earthquake Engineering and Seismology*. Geneva. 3-8 September.

Krawinkler H., Seneviratna GDPK. 1997. Pros and cons of a pushover analysis of seismic performance evaluation. *Engineering Structures*. 20(4-6). 452 – 464.

Lagomarsino S., Penna A., Galasco A., Cattari S. 2013. TREMURI program: an equivalent frame model for the nonlinear seismic analysis of masonry buildings. *Engineering Structures*. 56. 1787 – 1799.

Magenes G., Penna A. 2009. Existing masonry buildings: general code issues and methods of analysis and assessment. *Proc. of Eurocode 8 perspectives from the Italian Standpoint Workshop*. Napoli, Italy.

Magenes G., Penna A., Senaldi I., Rota M., Galasco A. 2014. Shaking table test of a strengthened full-scale stone masonry building with flexible diaphragms. *International Journal of Architectural Heritage: Conservation, Analysis, and Restoration*. 8(3). 349 – 375.

Mendes N., Lourenço PB. 2009. Seismic assessment of "Gaioleiro" buildings in Lisbon, Portugal. *Journal of Earthquake Engineering*. 14(1). 80 – 101.

Penna A., Lagomarsino S., Galasco., A. 2014. A nonlinear macroelement model for the seismic analysis of masonry buildings. Earthquake Engineering and Structural Dynamics. 43(2). 159 – 179.

Vidic T., Fajfar P., Fischinger M. 1996. Consistent inelastic design spectra: strength and displacement. *Earthquake Engineering and Structural Dynamics*. 23. 507 – 521.